A facile approach to modify cellulose nanocrystal for the adsorption of perfluorooctanoic acid

Chaimaa Gomri, Belkacem Tarek Benkhaled, Arnaud Chaix, Christophe Dorandeu, Joel Chopineau, Eddy Petit, Karim Aissou, Didier Cot, Marc Cretin, Mona Semsarilar

A Facile Approach to Modify Cellulose Nanocrystal for the Adsorption of Perfluorooctanoic acid

Chaimaa Gomri [a], Belkacem Tarek Benkhaled [a], Arnaud Chaix [a], Christophe Dorandeu[b], Joel Chopineau[b], Eddy Petit [a], Karim Aissou[a], Didier Cot[a], Marc Cretin [a], Mona Semsarilar [a].

[a] Institut Européen des Membranes-IEM (UMR 5635), Univ Montpellier, CNRS, ENSCM, 34095 Montpellier, France

[b] ICGM, Univ. Montpellier, CNRS, ENSCM, Montpellier, France.

Abstract

Cellulose-based materials are a sustainable alternative to polymers derived from petroleum. Cellulose nanocrystal (CNC) is a biopolymer belonging to this family; it is commonly known for its important physical and chemical properties and ability to form a film. Modifying CNC *via* electrostatic interaction provided by cationic polymers is a facile and promising technique to enlarge the application of CNC. Herein, we report the preparation of films, from blends of negatively charged CNC and positively charged poly (trimethyl aminoethyl methacrylate) (PTMAEMA). The interaction between CNC and PTMAEMA was verified by using a quartz crystal microbalance with dissipation monitoring (QCM-D), as well as by measuring the particle size and ζ-potential of the casting mixture. To favor the application of the nanocomposite film in water treatment, the film was supported on Whatman™ paper, and adsorption tests were conducted using perfluorooctanoic acid (PFOA) as a model compound for the family of persistent fluorinated pollutants known as PFAS (per- and polyfluoroalkyl substances).

Keywords

Cellulose Nanocrystal (CNC); Perfluorooctanoic acid (PFOA); Adsorption; Poly (trimethyl aminoethyl methacrylate) (PTMAEMA); Reversible Addition-Fragmentation chain Transfer (RAFT).

1. Introduction

Cellulose is an abundant crucial raw material able to meet the increasing demand for biodegradable and biocompatible materials. Cellulose has been used for many decades in the clothes and paper industries. In recent years, the exploitation of crystalline cellulose, also called cellulose nanocrystals “CNC”, increased thanks to their important mechanical properties and modifiable surface, while being eco-friendly (Trache, Hussin, & Thakur, 2017).

Commercial application of CNC depends on their quality which is defined by the extraction technique used. Several approaches can be applied to extract CNC from raw cellulose, such as the oxidation method, mechanical treatment, and acid hydrolysis. Extraction by acid hydrolysis requires the use of a strong acid which can be mineral or organic (Trache, Hussin, & Thakur, 2017). Using sulfuric acid for extraction leads to incorporating a negative surface charge due to the presence of sulfate groups (Gomri et al., 2022). The number of sulfate groups incorporated depends on the acid concentration and the hydrolysis time. These negatively charged sulfate groups endow cellulose with considerable reactivity that would allow surface modification via noncovalent interaction. Many researchers emphasize the outstanding properties of the modified CNC via noncovalent interaction with other materials such as polymers, surfactants, counter ion salts, and metals (Trache, Hussin, Haafiz, et al., 2017).

For instance, Engkagul et al. developed a nanocomposite film based on CNC combined with the cationic poly[(2-(methacryloyloxy)ethyl) trimethylammonium chloride] (PMETAC). It was shown that the incorporation of CNC into PMETAC increased the material's mechanical properties, assuming this is directly related to the pronounced electrostatic interaction between the two components (Engkagul et al., 2021). Surface functionalization of negatively charged CNC in an aqueous medium with positively charged polymer results in stable suspension. In another example, Khandal et al. showed how a noncovalent modification of CNC with negatively charged polyethyleneimine (PEI) could be efficient, leading to the formation of a stable suspension with interesting rheological behavior (Khandal et al., 2019).

The use of CNC in material science is limited since it disperses poorly in polymer matrices. To overcome this issue, Bondeson & Oksman modified CNC with a surfactant (acid phosphate ester of ethoxylated nonylphenol) to enhance its mixing in polylactic acid (PLA). The surfactant covered the surface of the CNC, hindering the formation of aggregates brought about by the formation of hydrogen bonds between CNCs (Bondeson & Oksman, 2007).

One practical application of modified CNC is their use as an adsorbent for water pollutants. Ranjbar et al. modified CNC with a positively charged surfactant (CTAB) to remove Congo red from an aqueous medium. The adsorption capacity of the developed material was as high as 244 mg g^{-1}, assuming that the adsorption process is governed by electrostatic attraction, hydrogen bonding, and hydrophobic attraction (Ranjbar et al., 2020). Cationic dyes such as methylene blue and malachite green were adsorbed using hybrid nanocomposite material based on CNC ($Cr(OH)_3$-NPs-CNC). The maximum adsorption capacities for both pollutants were respectively 106 mg g^{-1} and 104 mg g^{-1} (Nekouei et al., 2017). Besides organic dyes, modified CNC was applied to remove other contaminants such as arsenic (Dong et al., 2020), heavy metals (Hu et al., 2018), polyphenols (Asante et al., 2020), antibiotics (Liu et al., 2020), etc.

Currently, the pollutants of increasing concern to researchers are per- and polyfluoroalkyl substances (PFAS). PFAS are organic compounds that are fully or partially fluorinated. The strong bond between carbon and fluorine endows PFAS with high thermal and chemical stability enabling their extensive use in many fields (Lu et al., 2020). These pollutants have been increasingly detected in the aquatic systems presenting a real threat regarding their toxicity. Two main processes are used to remove PFAS from water: separation and degradation. Adsorption is a separation method commonly used to remove PFAS and has shown its efficiency (Wanninayake, 2021). Thus, green adsorbents such as activated carbon, biochar, polysaccharide-based materials, and aminated sorbents are promising for PFAS remediation (Militao et al., 2021).

In this study, we use a facile approach to modify CNC with positively charged poly(trimethylaminoethyl) methacrylate (PTMAEMA) to remove PFAS. For that PTMAEMA was first synthesized using Reversible Addition-Fragmentation chain Transfer (RAFT). The attachment of the PTMAEMA to CNC and the interaction between them were investigated using a quartz crystal microbalance with dissipation monitoring (QCM-D). Film based on PTMAEMA and CNC was prepared using Whatman ™ filter paper as a support to increase the mechanical stability of the final adsorbing surface. The resulting nanocomposite film was used to remove perfluorooctanoic acid (PFOA) from an aqueous solution. PFOA was used as a model compound from the PFAS family. The adsorption capacity of the developed composite film was evaluated using high-performance liquid chromatography coupled with mass spectroscopy (HPLC-MS).

In the present work, the assumption is that, due to the nature of CNC (presence of surface negative charge), functional polymer chains could be easily attached to their surface using electrostatic charges. The surface of the CNC is modified using a well-defined functional polymer via ionic-interactions, so the functional material could be used for adsorption and removal of pollutants as illustrated in figure 1.

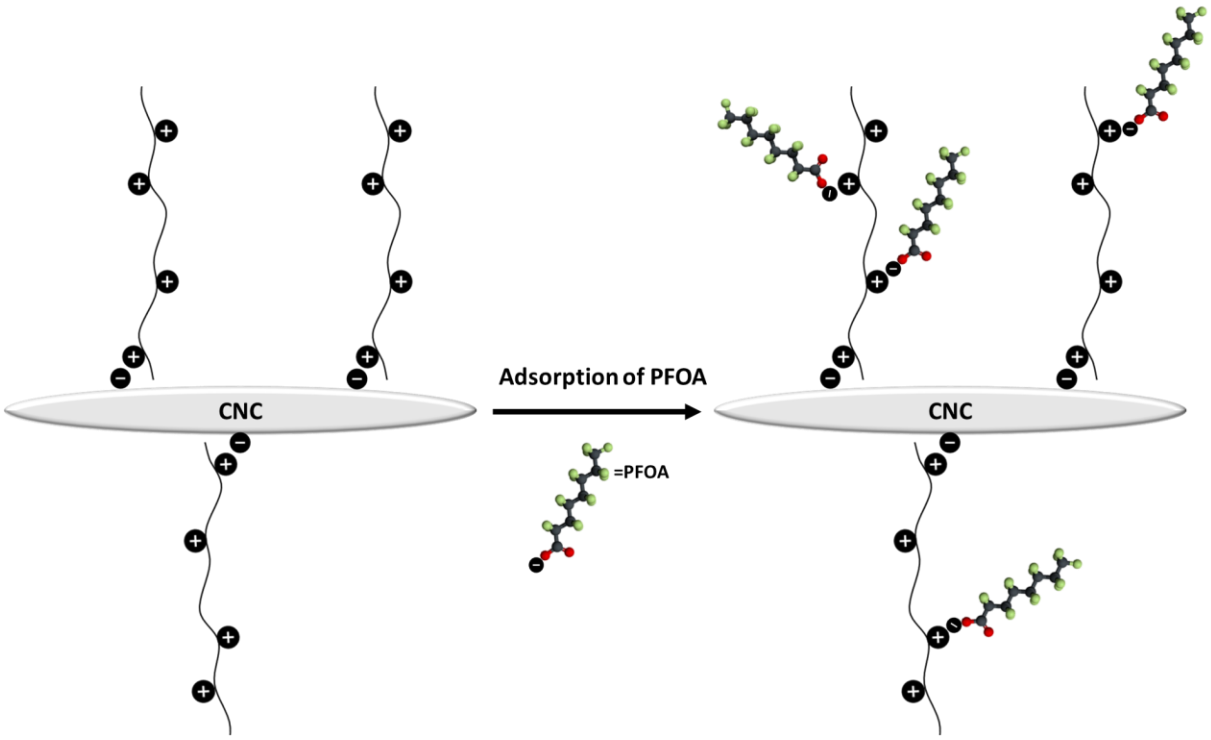

Figure 1. Illustration of the adsorption of PFOA onto non-covalently modified CNC

2. Materials and methods

2.1. Materials

Cellulose nanocrystal was kindly provided by CelluForce Inc. All reagents were purchased from Sigma-Aldrich and used without further purification. Dimethylamino ethyl methacrylate" DMAEMA" was used as the monomer, 4-Cyano-4-(phenylcarbonothioylthio)pentanoic acid was used as the RAFT agent and recrystallized 2,2'-azobisisobutyronitrile (AIBN) was used as the initiator. Tetrahydrofuran (THF) was used as solvent for the polymerization. Hexane was used for the precipitation of the polymer. Iodomethane was used to quaternize the amine of the polymer. $CDCl_3$ was used as a NMR solvent, and Whatman™ paper was used to support the developed material.

2.2. Synthesis of Poly (trimethyl aminoethyl methacrylate) "PTMAEMA."

Poly (dimethylamino ethyl methacrylate) was first synthesized by reversible addition−fragmentation chain transfer (RAFT). 2-(Dimethylamino) ethyl methacrylate (5 g, 31.80 mmol), 4-cyano-4-(phenylcarbonothioylthio)pentanoic acid (0.13 g, 0.4 mmol) and azobisisobutyronitrile (0.015 g, 0.09 mmol) were dissolved in tetrahydrofuran (5 mL) in a round-bottomed flask. The sealed reaction vessel was purged by bubbling nitrogen. The reaction mixture was stirred for 24 h at 70 °C. The resulting polymer (monomer conversion = 94 %, M_n = 2499, M_w = 2623, and $Đ$ =1.05) was purified by precipitation in hexane. The degree of polymerization was calculated using ^{1}H NMR spectroscopy by comparing the integral of the signals corresponding to the aromatic protons of the RAFT agent (7.5-8 ppm) with signals corresponding to CH_2 of the polymer backbone (3.87 ppm; 4.52 ppm). To quaternize the amine, the synthesized polymer was dissolved in water and placed into an ice bath, then CH_3I was added dropwise, and the mixture was kept under stirring for 2 h. The final product was then freeze-dried. Quaternization was confirmed using ^{1}H NMR by comparing the integral of the signals corresponding to the proton of the amine before and after the modification. The obtained yield was 100%.

2.3. Investigation of CNC and PTMAEMA interaction.

To investigate the interaction of CNC and PTMAEMA, nanocomposite films were prepared using different concentrations of PTMAEMA, as shown in Table 1. First, 0.4 g of CNC was dispersed in 15 mL of deionized water and sonicated for 30 min. Then 5mL of aqueous PTMAEMA solution with different concentrations was mixed with CNC solution and stirred for 24h at room temperature. The mixtures were poured into a stainless mold and dried at room temperature.

Samples references	CNC	CNC:PTMAEMA 1	CNC:PTMAEMA 2	CNC:PTMAEMA 3	CNC:PTMAEMA 4
PTMAEMA: CNC (Molar Ratio)	0	1	0.5	0.25	0.1

Table 1. Composition of the nanocomposite films

2.4. Preparation of supported CNC/PTMAEMA film

To test the efficiency of CNC/PTMAEMA film in removing perfluorooctanoic acid (PFOA) from an aqueous solution; CNC and PTMAEMA were deposited consecutively on cellulose filter paper (Whatman™) by spin coating to ensure a homogeneous deposit since the blend of CNC and PTMAEMA was too viscous. First, the cellulose filter paper was soaked for 24 h in NaOH solution, rinsed, and then dried at room temperature. Then, 0.5 mL of CNC aqueous solution (2% w/v) was spin-coated (100 rpm-120 s) on cellulose filter paper (diameter = 4.7 cm) and dried for 15 min at 70 °C in the oven. At the second step, 0.5 mL of PTMAEMA aqueous solution (2% w/v) was spin-coated (100 rpm, 120 s) on the cellulose filter paper coated with CNC. These steps have been repeated two times to ensure proper blending of CNC and PTMAEMA. The obtained composite film was cut into pieces (20 mg) and used for the PFOA adsorption experiments.

2.5. PFOA adsorption experiments

Adsorption experiments were conducted at room temperature. 20 mg (1 cm^2) of the composite film was placed in a beaker containing 50 mL PFOA (aq.) solution of 10 ppm (pH = 6.5). The solution was stirred for 6 days, and samples were taken at different time intervals. The adsorption kinetics were analyzed by pseudo-first order model and pseudo-second order model by fitting the experimental data into their linear form consecutively (Eq. 1) and (Eq. 2):

$$\ln(q_e - q_t) = \ln(q_e) - K_1 t \quad \textit{(Eq.1)}$$

$$\frac{t}{q_t} = \frac{1}{K_2\, q_e^2} + \frac{t}{q_e} \qquad \textit{(Eq.2)}$$

Where q_e is defined as the equilibrium adsorption capacity, K_1 (min^{-1}) is the constant of the pseudo-first order model, and K_2 (g mg^{-1} min^{-1}) is the constant of the pseudo-second order model.

A concentration ranging from 1 to 100 ppm of PFOA was used to investigate adsorption isotherms based on Langmuir and Freundlich model. Langmuir model considers monolayer adsorption of the adsorbate and homogeneous distribution of the adsorption site. The following equation presents the linear form:

$$\frac{C_e}{q_e} = \frac{C_e}{q_m} + \frac{1}{q_m K_L} \qquad \textit{(Eq.3)}$$

Where C_e is the concentration at the equilibrium, q_e is the quantity adsorbed at the equilibrium, q_m is the maximum quantity adsorbed, and K_L is the Langmuir constant.

Freundlich model considers the binding sites of the adsorbent heterogeneous, and the adsorption is multilayer. The following equation presents the linear form:

$$\ln(q_e) = lnK_f + \frac{1}{n} lnC_e \qquad (Eq.4)$$

Where K_f is a Freundlich constant, and $\frac{1}{n}$ is the heterogeneity factor.

2.6. Characterization

Particle size and ζ-potential were measured using Anton-Paar Litesizer 500 at 20°C. Samples were prepared at a concentration of 2 w/v %.

FT-IR analysis was made on a Thermo Nicolet Nexus FTIR spectrometer with a diamond ATR attachment. Samples were subjected to 32 scans in the range of 4000 cm^{-1} and 650 cm^{-1}, with a resolution of 4 cm^{-1}.

Thermogravimetric analysis (TGA) was conducted using TA instruments SDT Q600 by heating the sample to 700 °C under nitrogen with a 10°C/min ramp.

Transmission Electron Microscopy (TEM) images were obtained using JOEL 1400 flash. Samples were prepared at 0.1% (w/v) and placed on a carbon-coated copper grid for 60 seconds, then ammonium molybdate was added for 20 s to stain the samples. The grid was then dried using a vacuum hose.

Proton nuclear magnetic resonance (NMR) analysis was conducted on a Bruker Advance spectrometer 400 MHz at room temperature using $CDCl_3$ as solvent.

Size exclusion chromatography (SEC) was performed on TDA 305, Malvern Instruments Worcestershire, UK. The instrument was equipped with a two-column set-up with a particle size of 5 µm, and containing a refractive index detector (RI, concentration detector). The eluent was tetrahydrofuran (THF) with a flow rate of 1.0 mL min^{-1}. OmniSEC software (version 10, Malvern Panalytical, Malvern, UK) was used to analyze the data.

X-ray diffraction (XRD) analysis was performed on an X'pert Pro (PAN Analytical). The analysis was done in the 2θ range from 4° to 60°. The crystallinity index was calculated using deconvolution method. Crystalline peaks were extracted using a software (OriginPro; Peak deconvolution). Gaussian function was used for the curve fitting. Crystallinity index was calculated by dividing the area of all crystalline peaks on the total area (Schroeder et al., 2010).

Atomic force microscopy (AFM Nano-Observer, CSInstruments) was used in tapping mode to characterize the surface morphology of unblended and blended CNC films. Silicon cantilevers (PPP-NCH, Nanosensors) with a typical tip radius of ~5 nm was used. The resonance frequency of the cantilevers was about 235 kHz.

Scanning electron microscopy (SEM, Hitachi S-4800) was used at an accelerating voltage of 5 kV to acquire top view and cross-section images of unblended and blended CNC films.

The contact angle was measured using the Digidrop instrument (GBX scientific LTD, Dublin, Ireland). 5 µL of deionized water was deposited onto the films. The contact angle was measured using Digidrop software based on the recorded image.

Quartz crystal microbalance with dissipation monitoring (QCM-D) E1 was provided by Biolin Scientific (Västra Frölunda, Sweden). The instrument was equipped with a quartz crystal sensor with a silica-coated surface resonating at 5 MHz. The sensor was coated with CNC, and the flow chamber was fed by an aqueous solution of PTMAEMA.

QCM-D provides information on the adsorption kinetics, adsorbed mass, and elastic properties of the layer adsorbed at the sensor's interface. The quartz crystal oscillates at a constant frequency. By varying the mass of the crystal, the resonance frequency of the oscillation changes. This change in frequency could be converted to the adsorbed mass using the Sauerbrey equation (see experimental section for details).

$$m = C(\Delta f \times n^{-1}) \quad \textit{(Eq.5)}$$

Where C is a sensitivity constant ($C = -0.177\ (mg\ m^{-2})Hz^{-1}$. Δf (Hz) corresponds to the change in resonance frequency, and n is the overtone ($n = 1,3,\dots,11$). In this experiment, results from the fundamental overtone have been exploited.

QCM-D also provides information about viscoelasticity, thickness, and water content of the adsorbed layer by measuring the dissipation (D). Dissipation measure is based on the time the oscillating crystal takes to stop when the experiment is finished.

PFOA adsorption was evaluated by High-performance liquid chromatography coupled to mass spectroscopy (HPLC-MS). The instrument was equipped with Waters-Xselect HSST3 100mm × 2.1 mm column with 2.5 µm particle size. The mobile phase consists of Buffer A (water + 0.1% formic acid) and Buffer B (acetonitrile + 0.05% formic acid) with a constant flow rate of 0.25 mL min^{-1}.

I- Synthesis of poly (trimethyl aminoethyl methacrylate) "PTMAEMA" by RAFT polymerization.

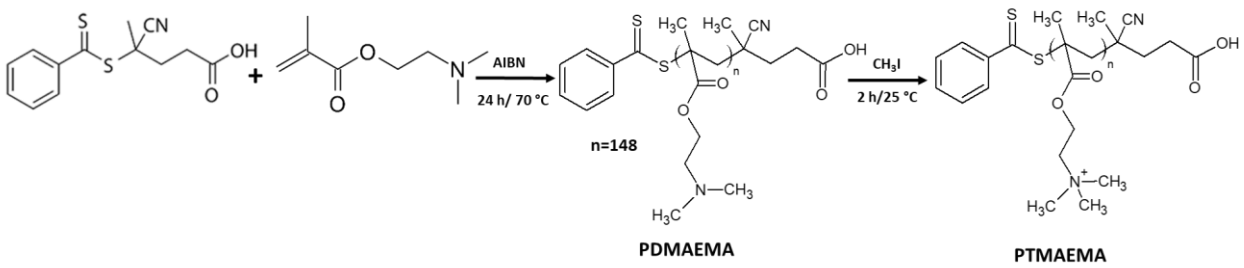

II- Preparation of nanocomposite film based on CNC and PTMAEMA for the adsorption of PFOA.

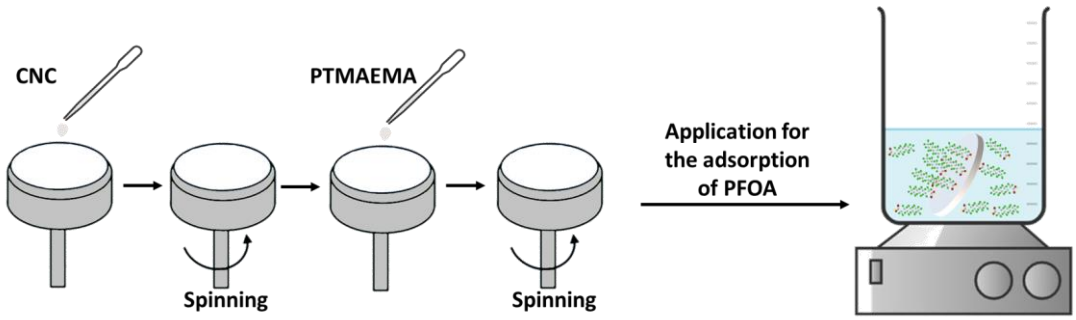

Figure 2. Schematic illustration of the preparation of the nanocomposite film and its application for the adsorption of PFOA

3. Results and discussion

3.1. Structural characteristics of CNC

CNC is mainly isolated from cellulose fibers through acid hydrolysis. This acid treatment hydrolyzes the disordered regions but retains the crystalline regions with a rod-like morphology (Figure 3.a). When sulfuric acid is used for extraction, it introduces negatively charged sulfate esters groups on the surface of the CNC. These negative charges endow CNC with a good dispersity in water but compromise its thermo-stability (Habibi et al., 2010). Acid concentration directly impacts the size of CNC particles so that increasing acid concentration reduces their diameter, length, and width; it also impacts the percent of sulfate groups inserted (H. Zhang et al., 2019). Because of this, the CNC used in this work was thoroughly analyzed. Elemental analysis, indicated 0.75% of sulfur atoms, and the TGA analysis indicated a good thermally stable microcrystalline cellulose, since the main degradation occurred between 260°C-400°C (Figure 3.c) (H. Zhang et al., 2019).

FT-IR analysis (Figure 3.b) showed a large band at 3271 cm^{-1} corresponding to O-H stretching vibration. The band at 2892 cm^{-1} corresponds to the stretch of C-H. The peak at 1644 cm^{-1} is attributed to O-H bending vibration related to water present in CNC due to its hydrophilic nature. The intensity at 1428 cm^{-1} is associated with CH_2 bending vibration. Band related to C-C forming the cycle appeared at 1159 cm^{-1}, and the broad peak at 1061 cm^{-1} is attributed to the stretching vibration of C-O (H. Zhang et al., 2019) (Hemmati et al., 2018) (Oyewo et al., 2019).

The XRD profile of CNC is presented in figure 3.d. The result shows three main peaks at 2Θ=34.7°, 22.7°and 15.8°. Each peak is related to respectively following crystalline planes (110), (200), and (004), as described by (Sun et al., 2016). By using the deconvolution method (Figure S1), the obtained crystallinity index is 36.26%.

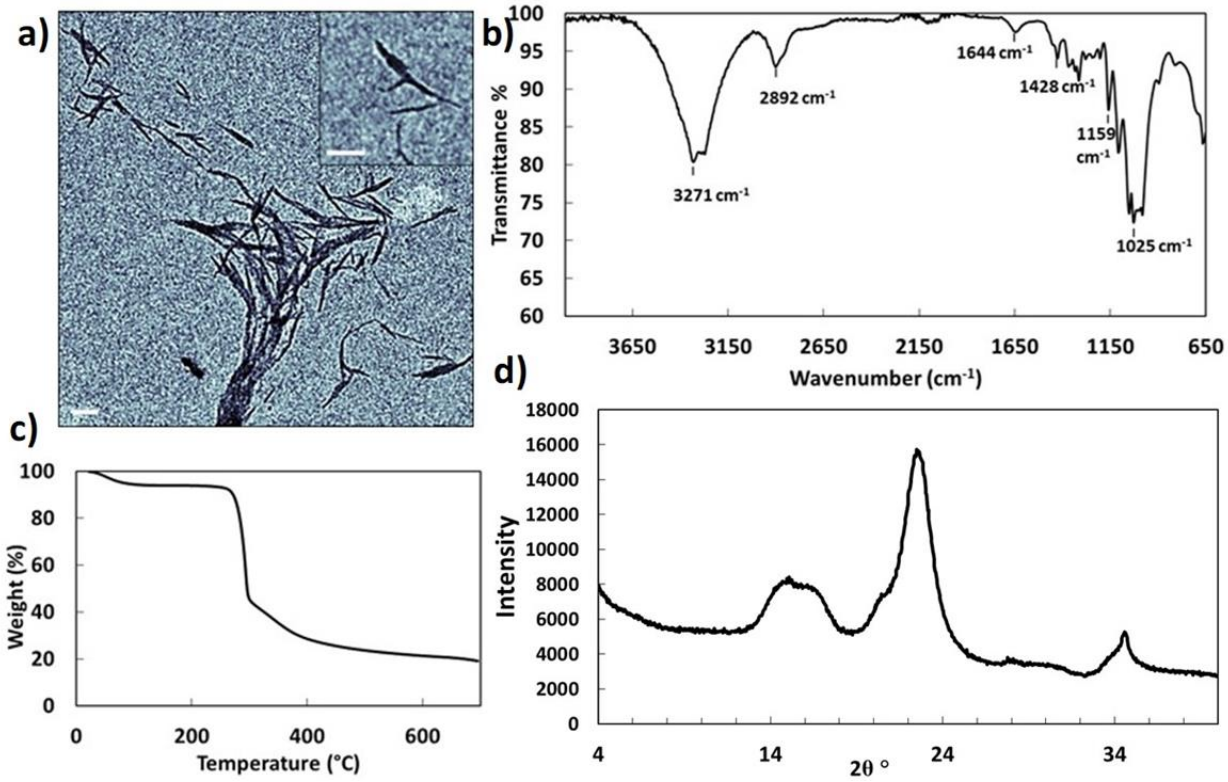

Figure 3. a) TEM image, scale bars= 1 μm, b) FTIR pattern, c) TGA, and d) XRD pattern of CNC

3.2. Characterization of synthesized PTMAEMA

The controlled polymerization of DMAEMA was performed *via* RAFT polymerization with a conversion rate of 94% resulting in an average molecular weight of 11 500 g mol^{-1} and dispersity index ($Đ$) of 1.05 (Figure 4.a). The amine groups of PDMAEMA were then quaternized using iodomethane to provide permanent positive charge. The modification was confirmed by NMR. As seen in figures (4.c and d), there is a clear shift of the peak corresponding to the proton of N-$(CH_3)_2$ from 2 to 3 ppm. The FTIR analysis of PTMAEMA (figure 4.b) showed a band at 3440 cm^{-1} related to water adsorption due to the hydrophilic nature of the polymer (Yin et al., 2017). Peaks at 3000 and 2950 cm^{-1} correspond to the C-H bond in CH_2 and -N$(CH_3)_3$. The band at 1722 cm^{-1} corresponds to the C=O stretching and the characteristic peak of the C-N at 1138 cm^{-1}.

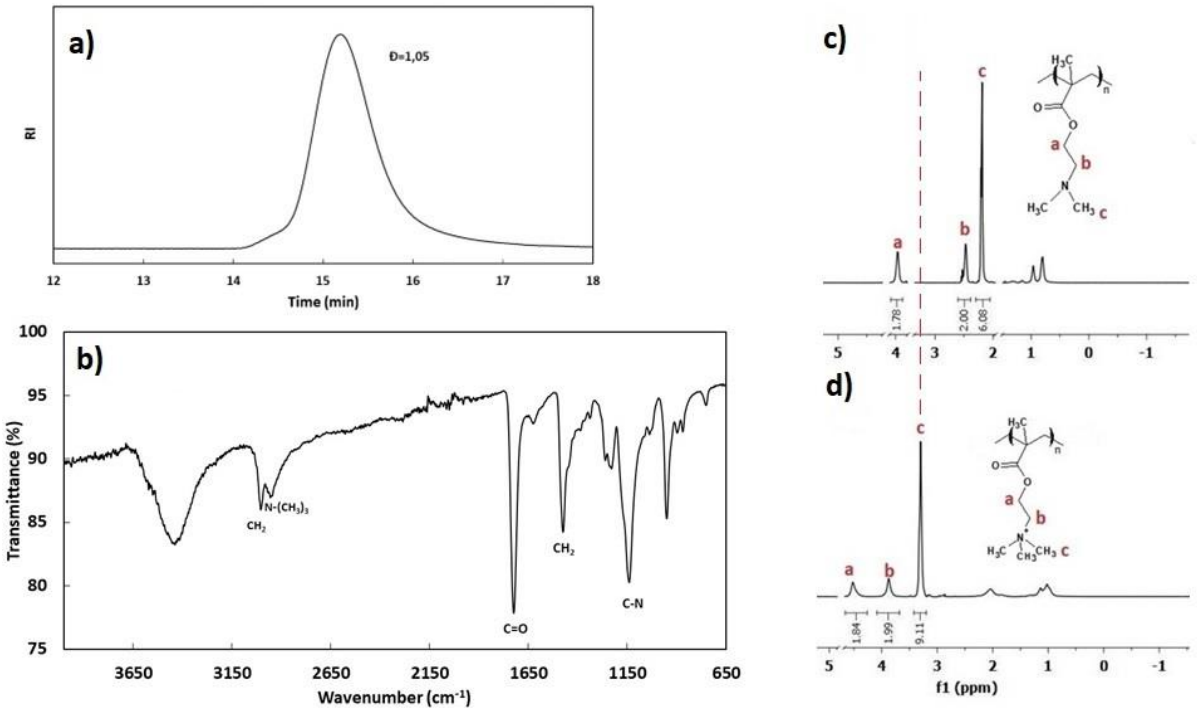

Figure 4. a) SEC trace for PDMAEMA in THF, b) FTIR pattern of PTMAEMA, c) NMR spectra of PDMAEMA (before quaternization), and d) PTMAEMA (after quaternization)

3.3. Investigation of the interaction between CNC and PTMAEMA

To investigate the interaction between CNC and PTMAEMA, the ζ-potential of an aqueous dispersion of CNC with different PTMAEMA concentrations was measured. The obtained results are presented in figure 5. The initial ζ-potential value of aqueous dispersion of CNC before adding PTMAEMA was -67 mv. As PTMAEMA was added, the ζ-potential value increased until it reached a positive value of 44 mV. This ζ-potential value (> 30 mV) indicates the formation of stable dispersions of CNC and PTMAEMA as reported by Rowen and co-workers (Engkagul et al., 2021). Besides the stability, this positive value indicates that the PTMAEMA chains are attached to the CNC surface via strong electrostatic interactions, covering the surface of CNC crystals.

The TEM image analysis has been carried on 100 bare CNC particles before and after modification (figure S2). Before modification CNC presented a diameter of 11 nm and length of 153 nm at dry state (aspect ratio of 13.9), these dimensions remain unchanged after the CNCs have been modified with the charged polymer chains (figure S3). However, the DLS analysis (figure S4.a), suggests that 60% of particles forming CNC dispersion were about 1.23 µm. When adding an equivalent molar ratio of PTMAEMA, the size was reduced to 0.48 µm (figure S4.b). This is most

probably due to the attachment of the PTMAEMA chains to the surface of CNC providing enough same charge repulsion between the CNC particles, thus preventing aggregation. Lower amounts of added polymer (molar ratio of 0.1) resulted in formation of big aggregates (9.17 µm), suggesting that the surface of the CNC would need to be completely covered with the polymer as fewer positive charge result in large aggregates.

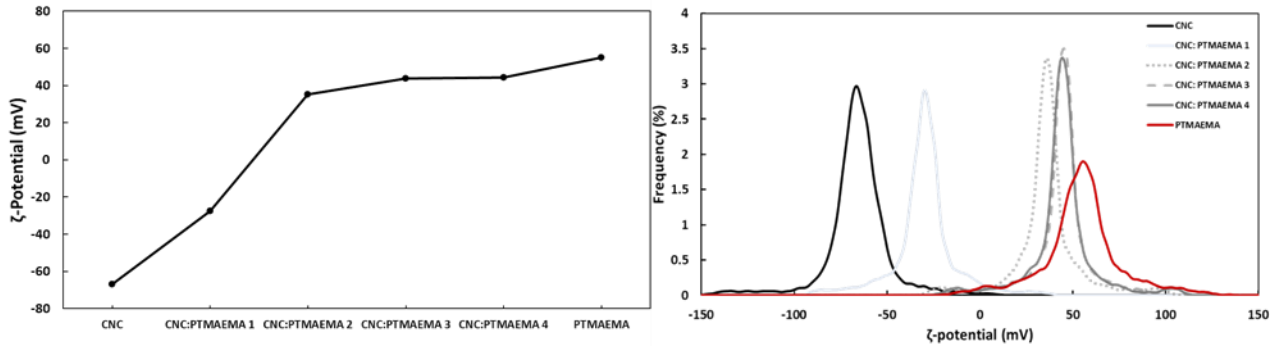

Figure 5. ζ-potential of the different CNC: PTMAEMA samples

To investigate the interaction between anionic CNC and cationic PTMAEMA, silica quartz crystal sensors were prepared following the same procedure as Engström et al. (Engström et al., 2021). CNC layer was deposited on clean QCM-D crystal by spin coating (3000 rpm for 120 s). Then the sensor coated with CNC was equilibrated overnight in water to ensure a stable baseline. For the experiment, an aqueous solution of PTMAEMA at 2 w/w % was introduced into the flow chamber with a constant flow rate of 0.1 mL min^{-1}. After reaching the equilibrium, deionized water was introduced into the chamber to remove the loosely attached polymer. The recorded frequency variation was 300 Hz which can be estimated, following the Sauerbrey model (Eq. 5), to an adsorbed mass of 53 mg m^{-2} (figure 6). This value highlights the strong electrostatic interaction between anionic CNC and cationic PTMAEMA. Moreover, the equilibrium was reached after only 3 minutes. The ratio $\frac{\Delta D}{\Delta f}$ gives information about the rigidity and the softness of the adsorbed polymer, which is related to the amount of water entrapped in the layer (Kontturi et al., 2008). The value obtained here was 0.38. Based on the result reported by Engström (Engström et al., 2021), the adsorbed polymer can be described as viscoelastic. The adsorption of PTMAEMA on the CNC surface was investigated by presenting the variation of the dissipation as a function of frequency (so-called $D - f$ plot) before the rinsing step (figure 7). When adding PTMAEMA, frequency and dissipation both increase forming a curve implying a slight change in conformation of PTMAEMA on the CNC surface.

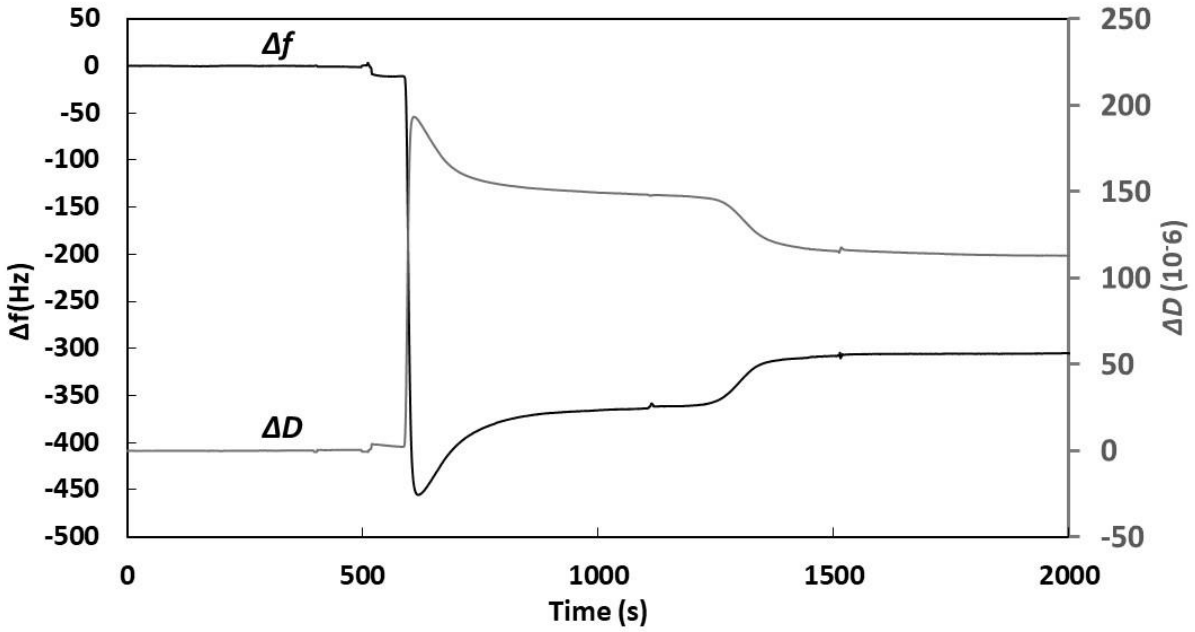

Figure 6. QCM-D analysis of the frequency (Δf) and dissipation (ΔD) observed for the fundamental overtone from adsorption of the aqueous solution of PTMAEMA on CNC.

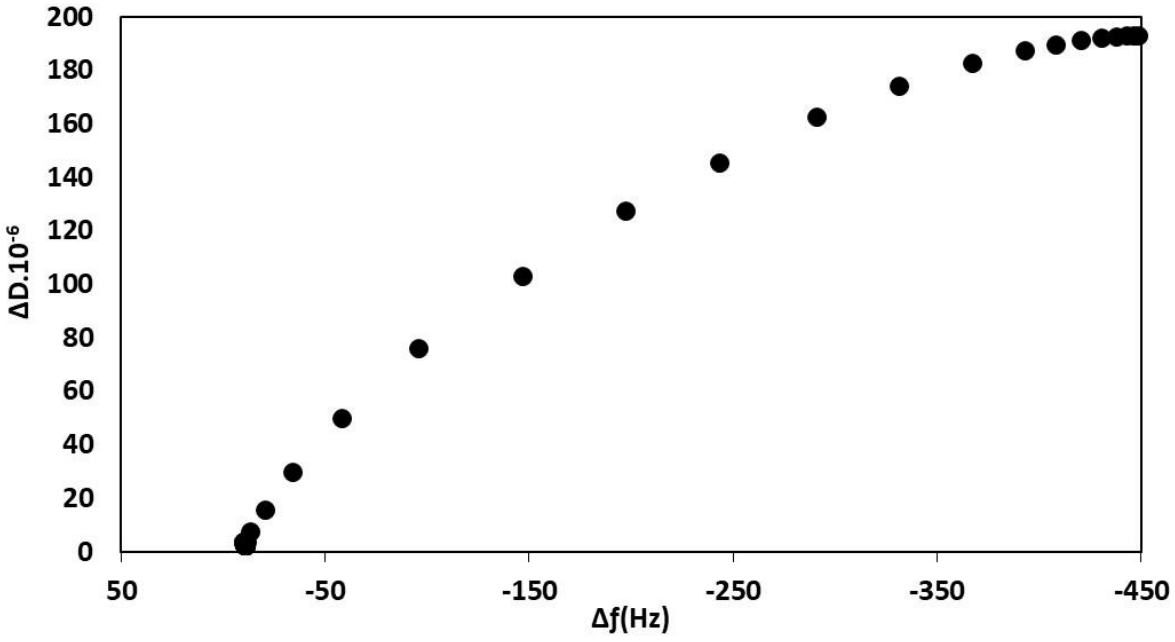

Figure 7. Variation of the dissipation as a function of frequency

CNC is known for its ability to form an iridescent well-structured film (figure 8). The SEM image presented in figure 9 shows the free surface of a neat CNC film formed by nano-rods having a high degree of alignment. Conversely, the

degree of nano-rod alignment is decreased within CNC films blended with PTMAEMA due to the electrostatic interactions between CNC and PTMAEMA (see Figure 9b). It is noteworthy that the high degree of nano-rod alignment on the top surface of the neat CNC film is associated with a lower surface roughness (R_{rms} = 15.9 nm) than that of the CNC: PTMAEMA 1 composite (R_{rms} = 53.8 nm), as revealed by the AFM topographic images presented in figure 10. In addition, the cross-sectional SEM image of the neat CNC film revealed the presence of a typical stacked layered structure that is not clearly observed within the CNC: PTMAEMA 1 composite (see Figure 11). This behavior is in accordance with the disappearance of the iridescent properties within the CNC: PTMAEMA (1:1) composite. The XRD scans of the CNC/PTMAEMA nanocomposite films (figure S5) showed that by adding PTMAEMA, the diffraction peaks of CNC get broadened even at low concentrations of PTMAEMA, indicating that the polymer covers the surface of CNC which hinders the appearance of well-defined CNC crystalline peaks. To evaluate the effect of PTMAEMA on the hydrophilicity of the film, the contact angle of the films was measured, as presented in figure 12. As expected, CNC film was hydrophilic with a contact angle of 58°. Enhancing the concentration of PTMAEMA slightly decreased the contact angle value to 45°. This decrease, although very small is directly related to the hydrophilic nature of PTMAEMA.

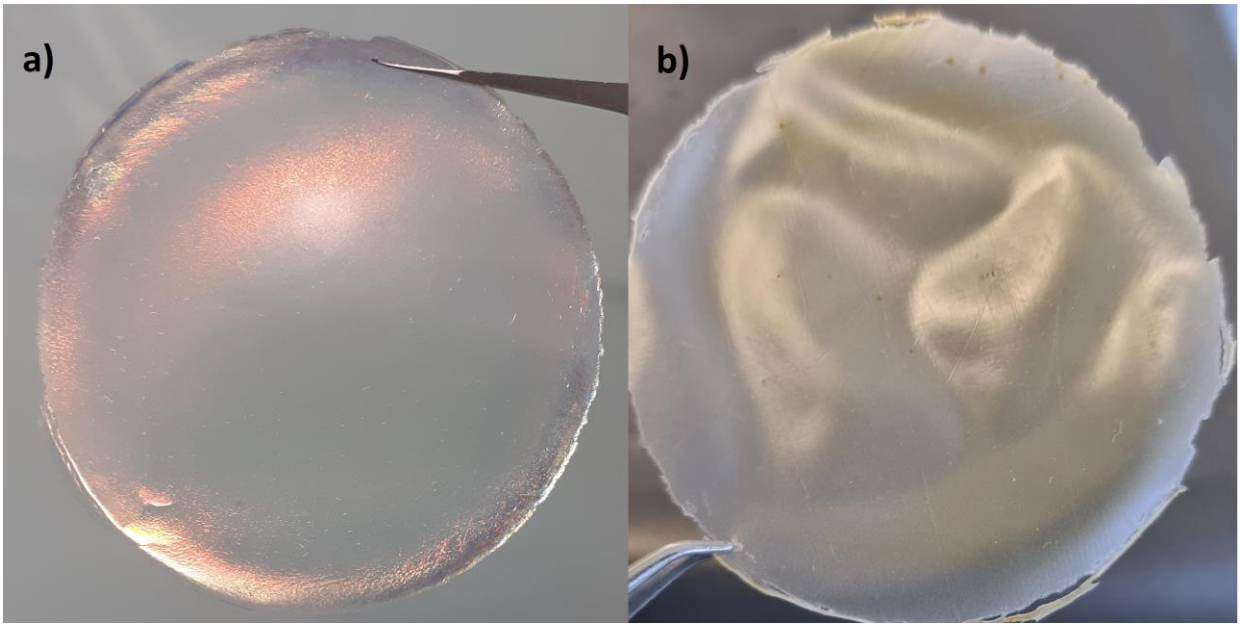

Figure 8. Films made of a) CNC and b) CNC blended with PTMAEMA

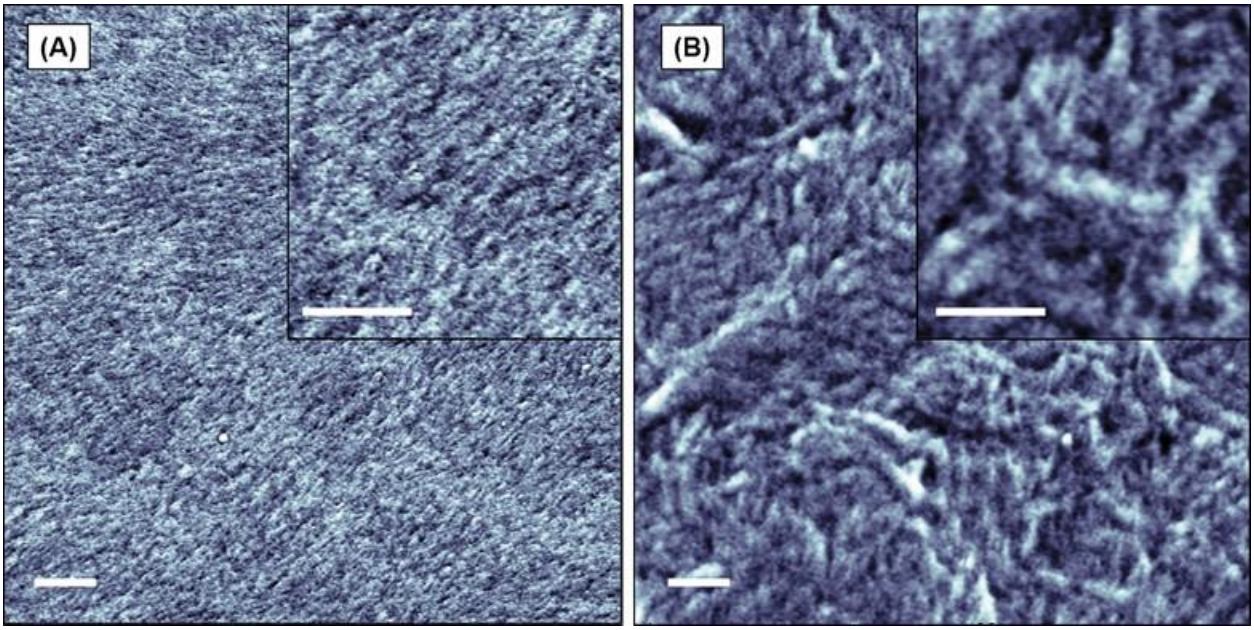

Figure 9. SEM images showing the representative top surface of (a) CNC and (b) CNC: PTMAEMA 1 films. Scale bars: 500 nm.

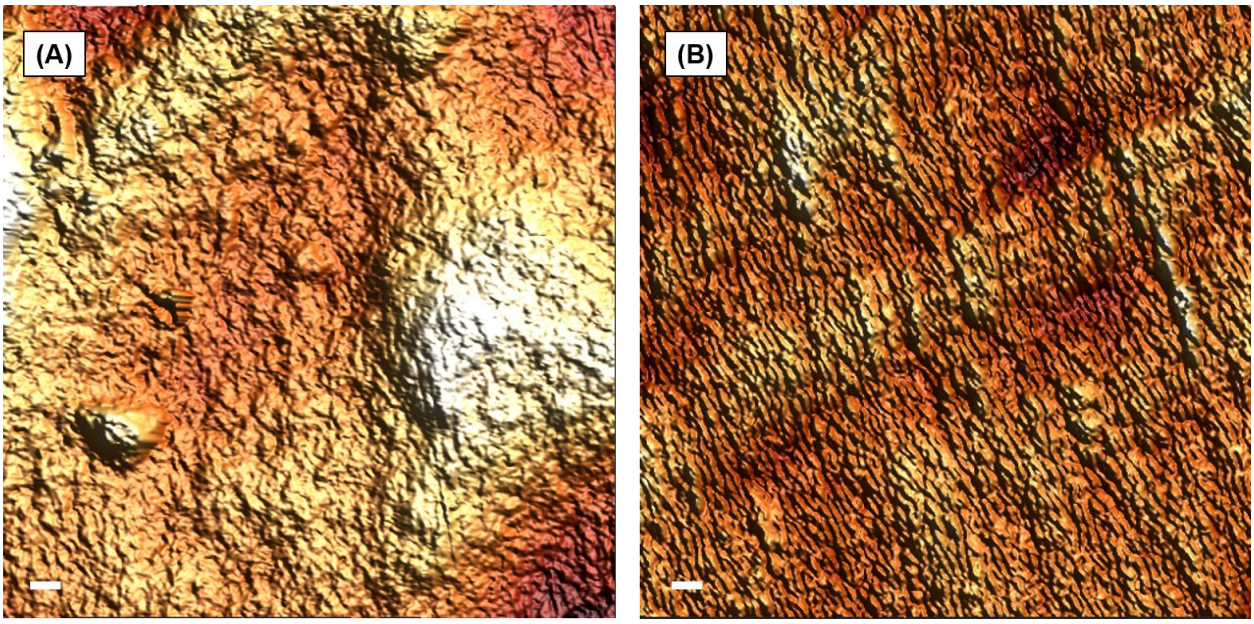

Figure 10. AFM topographic views showing the representative top surface of (a) CNC and (b) CNC: PTMAEMA 1 films. Scale bars: 500 nm.

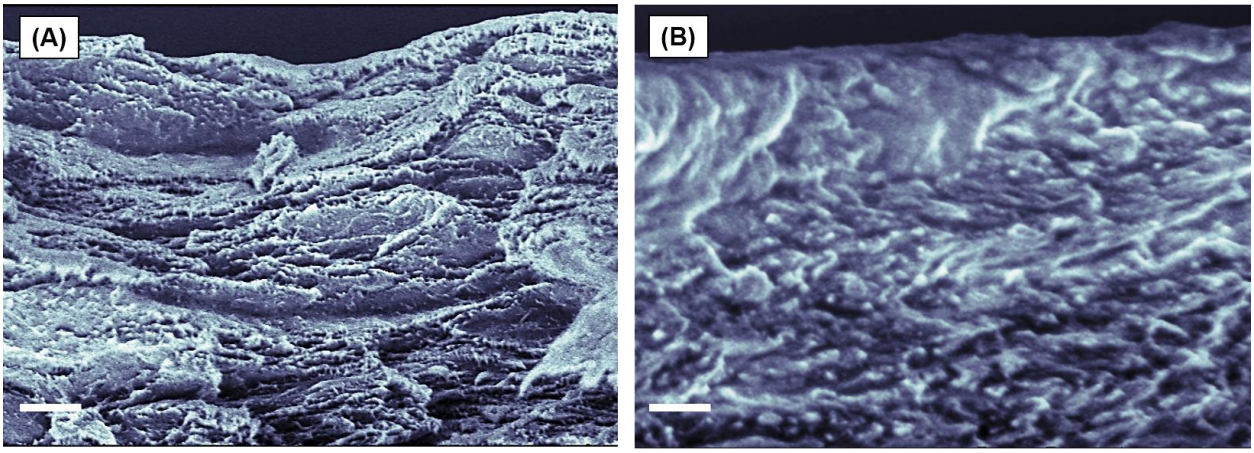

Figure 11. Cross-sectional SEM images showing the representative top surface of (a) CNC and (b) CNC: PTMAEMA 1 films. Scale bars: 500 nm.

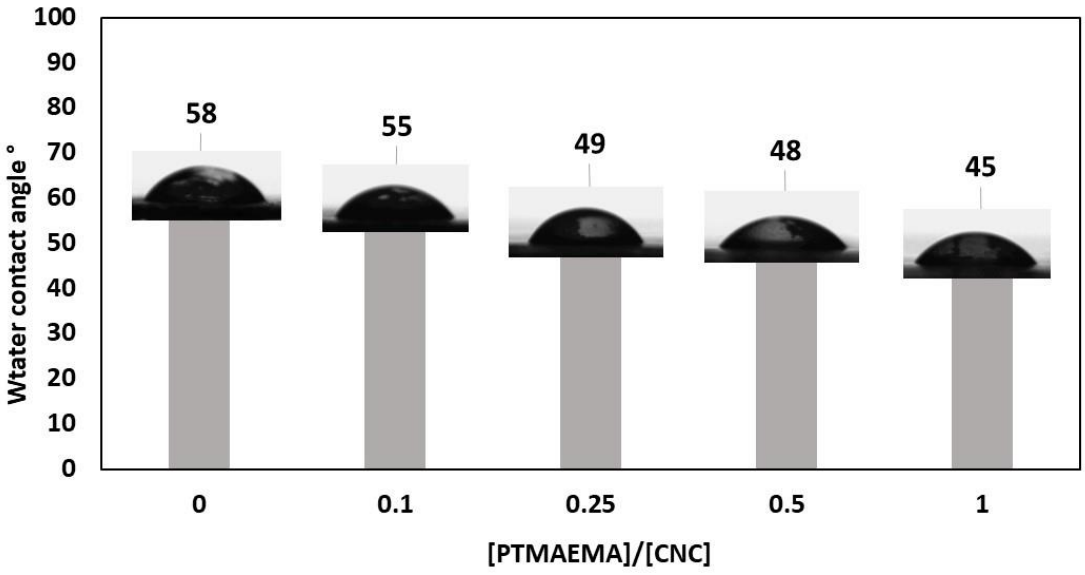

Figure 10. Variation of water contact angle as a function of the variation of the molar ratio of [PTMAEMA]: [CNC] between 0 and 1.

3.4. Evaluation of the stability of CNC/PTMAEMA based nanocomposite films.

In the previous paragraph we showed by QCM-D that the interaction between CNC and PTMAEMA is strong, that even after rinsing the coated sensor with water, PTMAEMA was still adsorbed on CNC. But this interaction doesn't keep the developed nanocomposite film from disintegrating when in water. This is because of the hydrogen bond that

is formed between water and the hydroxyl group of CNC. To overcome the disintegration of the film, Whatman™ paper was used as support. First, Whatman™ paper was soaked in aqueous solution of NaOH to activate it and favor its interaction with CNC. Then CNC and PTMAEMA were deposited on the cellulose filter paper consecutively by spin-coating. The deposition was confirmed by infrared (figure S6), a new peak that characterizes the carbonyl group of PTMAEMA appeared at 1722 cm^{-1}. To evaluate the efficiency of the developed material in removing PFOA, adsorption experiments were conducted in batch. Absorption test on bare Whatman™ paper was conducted as the control. As expected, no PFOA was adsorbed to the support Whatman™ paper.

The developed nanocomposite material showed great stability in an aqueous environment. The coated Whatman paper was still recoverable even after being placed in water for one week. Figure S7 presents the FTIR spectra of the modified Whatman™ paper after the adsorption of PFOA. The peak characterizing PTMAEMA was still present confirming that the material kept its integrity in water. Furthermore, we have the appearance of new peaks characterizing the adsorbed PFOA. The main advantage of this material is that its adsorption efficiency can be easily upgraded by carrying out a new deposition of the polymer. A small amount of polymer is needed for the coating, guaranteeing good results in the adsorption of PFOA. This material can be easily manufactured which makes it a good candidate to be used on a large scale.

3.5. Adsorption of PFOA onto CNC/PTMAEMA based nanocomposite films.

For a better understanding of the adsorption mechanism, the adsorption kinetic was investigated. Figure 13 represents the variation of C_t/C_0 as a function of time (h) for different concentrations of PFOA. For all the concentrations, the equilibrium is reached after 48 hours of the films being in contact with the PFOA solution. The adsorption efficiency of 100, 10 and 1 ppm of PFOA were 61%, 67%, and 76% respectively. Thus, increasing the concentration of PFOA led to a decrease in the removal efficiency.

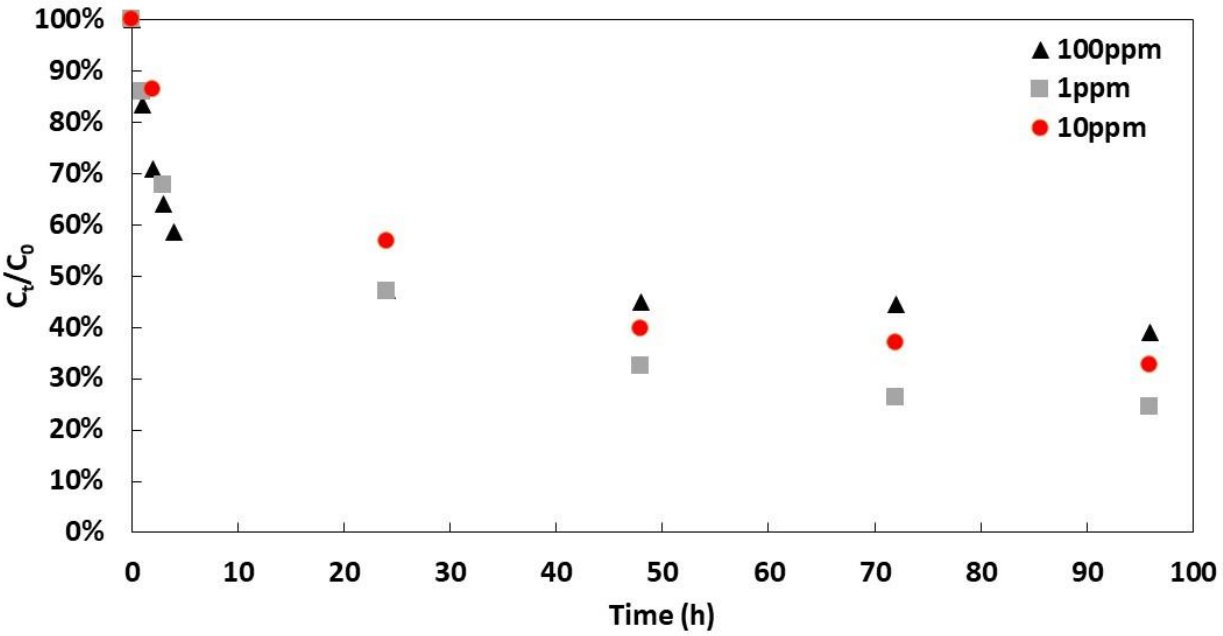

317

318 **Figure 11. Variation of C_t/C_0 as a function of time (h) for different concentrations of PFOA.**

319 To define the kinetic order and adsorption parameters, experimental data were fitted into equations (1) and (2). The
320 experimental results are presented in figure S8 and summarized in table 2. The pseudo-second order model was more
321 suited for the presented adsorption kinetics since the correlation coefficient was higher than the value obtained from
322 the pseudo-first order model (R^2= 0.99). The pseudo-second order model assumes that the rate-limiting step is
323 chemisorption, and the adsorption rate depends on adsorption capacity (Sahoo & Prelot, 2020), which correlates well
324 with the results obtained in figure 13, since for all the different concentrations the equilibrium is reached after 48
325 hours.

q_e experimental (mg g^{-1})	Pseudo-first order kinetic model			Pseudo-second order kinetic model		
	q_e (mg g^{-1})	K_1 (h^{-1})	R^2	q_e (mg. g^{-1})	K_2 (g mg h^{-1})	R^2
12.54	10.55	0.0372	0.95	13.42	0.0081	0.99

326 **Table 2. Adsorption kinetic parameters of PFOA**

327 A concentration ranging from 1 to 100 ppm of PFOA was used to investigate adsorption isotherms based on Langmuir
328 and Freundlich model. Based on the correlated coefficient "R^2" obtained for each model in table 3, Freundlich isotherm
329 best fitted the adsorption data, implying multilayer adsorption and the adsorption sites have different binding energies.

With 1/n being 0.854 (less than 1) implies a chemisorption process (Sahoo & Prelot, 2020). Langmuir isotherm did not fit as good as Freundlich isotherm, but it still can illustrate the maximum sorption which is 303.03 mg g^{-1}.

.

Langmuir model			Freundlich model		
q_m (mg g^{-1})	K_L (L g^{-1})	R^2	K_F (L g^{-1})	1/n	R^2
303.03	0.0146	0.75	5.08	0.8542	0.99

Table 3. Isotherm parameters of Langmuir and Freundlich model for the adsorption of PFOA

Comparing the obtained results to a similar study (D. Zhang et al., 2016) performed using granulated activated carbon (GAC) (K_2= 4.72 g mg h^{-1}) with the same initial concentration of PFOA (10 ppm), shows that the sorption rate obtained with modified CNC is higher (as sorption rate is inversely related to the rate constant "K_2"). Moreover, the maximum sorption indicated by the Langmuir model for modified CNC is 303.03 mg g^{-1} while for GAC is 52.8 mg g^{-1}(D. Zhang et al., 2016).

4. Conclusion

Modification of CNC surface is of such importance, since it broadens its application in different fields of science and technology, also enhances its compatibility with other materials. As hypothesized, CNC can be easily and efficiently modified via noncovalent interaction with oppositely charged moieties such as polymers. This modification is advantageous compared to covalent modification since it can be performed at large scales (industrial level). Herein we reported the modification of negatively charged CNC with a positively charged polymer (PTMAEMA). The collected data suggest that CNC and PTMAEMA interact with each other *via* strong electrostatic interactions, which results in formation of a stable suspension as well as a homogeneous film. For application in the adsorption of PFOA in an aqueous environment, Whatman™ paper was used to support the CNC- PTMAEMA film. The sorption kinetic best fitted the pseudo-second order model with a constant rate K_2= 0.0081 (g mg h^{-1}). The obtained results indicate that as assumed, the simple approach described here, is a viable pathway to prepare cheap and environmentally friendly material from CNC for efficient elimination of toxic PFAS from water.

5. REFERENCES

Asante, B., Sirviö, J. A., Li, P., Lavola, A., Julkunen-Tiitto, R., Haapala, A., & Liimatainen, H. (2020). Adsorption of bark derived polyphenols onto functionalized nanocellulose: Equilibrium modeling and kinetics. *AIChE*

Journal, *66*(2), 1–10. https://doi.org/10.1002/aic.16823

Bondeson, D., & Oksman, K. (2007). Dispersion and characteristics of surfactant modified cellulose whiskers nanocomposites. *Composite Interfaces*, *14*(7–9), 617–630. https://doi.org/10.1163/156855407782106519

Dong, F., Xu, X., Shaghaleh, H., Guo, J., Guo, L., Qian, Y., Liu, H., & Wang, S. (2020). Factors influencing the morphology and adsorption performance of cellulose nanocrystal/iron oxide nanorod composites for the removal of arsenic during water treatment. *International Journal of Biological Macromolecules*, *156*, 1418–1424. https://doi.org/10.1016/j.ijbiomac.2019.11.182

Engkagul, V., Rader, C., Pon, N., Rowan, S. J., & Weder, C. (2021). Nanocomposites Assembled via Electrostatic Interactions between Cellulose Nanocrystals and a Cationic Polymer. *Biomacromolecules*, *22*(12), 5087–5096. https://doi.org/10.1021/acs.biomac.1c01056

Engström, J., Reid, M. S., Brotherton, E. E., Malmström, E., Armes, S. P., & Hatton, F. L. (2021). Investigating the adsorption of anisotropic diblock copolymer worms onto planar silica and nanocellulose surfaces using a quartz crystal microbalance. *Polymer Chemistry*, *12*(42), 6088–6100. https://doi.org/10.1039/d1py00644d

Gomri, C., Cretin, M., & Semsarilar, M. (2022). Recent progress on chemical modification of cellulose nanocrystal (CNC) and its application in nanocomposite films and membranes-A comprehensive review. *Carbohydrate Polymers*, *294*(June), 119790. https://doi.org/10.1016/j.carbpol.2022.119790

Habibi, Y., Lucia, L. A., & Rojas, O. J. (2010). Cellulose nanocrystals: Chemistry, self-assembly, and applications. *Chemical Reviews*, *110*(6), 3479–3500. https://doi.org/10.1021/cr900339w

Hemmati, F., Jafari, S. M., Kashaninejad, M., & Barani Motlagh, M. (2018). Synthesis and characterization of cellulose nanocrystals derived from walnut shell agricultural residues. *International Journal of Biological Macromolecules*, *120*, 1216–1224. https://doi.org/10.1016/j.ijbiomac.2018.09.012

Hu, Z. H., Omer, A. M., Ouyang, X. K., & Yu, D. (2018). Fabrication of carboxylated cellulose nanocrystal/sodium alginate hydrogel beads for adsorption of Pb(II) from aqueous solution. *International Journal of Biological Macromolecules*, *108*, 149–157. https://doi.org/10.1016/j.ijbiomac.2017.11.171

Khandal, D., Riedl, B., Tavares, J. R., Carreau, P. J., & Heuzey, M. C. (2019). Tailoring cellulose nanocrystals rheological behavior in aqueous suspensions through surface functionalization with polyethyleneimine. *Physics*

of Fluids, *31*(2), 021207. https://doi.org/10.1063/1.5046669

Kontturi, K. S., Tammelin, T., Johansson, L. S., & Stenius, P. (2008). Adsorption of cationic starch on cellulose studied by QCM-D. *Langmuir*, *24*(9), 4743–4749. https://doi.org/10.1021/la703604j

Liu, J., Liu, D., Liu, S., Li, Z., Wei, X., Lin, S., & Guo, M. (2020). Preparation and Characterization of Sulfated Cellulose Nanocrystalline and its Composite Membrane for Removal of Tetracycline Hydrochloride in Water. *Energy and Environmental Materials*, *3*(2), 209–215. https://doi.org/10.1002/eem2.12055

Lu, D., Sha, S., Luo, J., Huang, Z., & Zhang Jackie, X. (2020). Treatment train approaches for the remediation of per- and polyfluoroalkyl substances (PFAS): A critical review. *Journal of Hazardous Materials*, *386*(December 2019), 121963. https://doi.org/10.1016/j.jhazmat.2019.121963

Militao, I. M., Roddick, F. A., Bergamasco, R., & Fan, L. (2021). Removing PFAS from aquatic systems using natural and renewable material-based adsorbents: A review. *Journal of Environmental Chemical Engineering*, *9*(4), 105271. https://doi.org/10.1016/j.jece.2021.105271

Nekouei, F., Nekouei, S., Keshtpour, F., Noorizadeh, H., & Wang, S. (2017). Cr(OH)3-NPs-CNC hybrid nanocomposite: a sorbent for adsorptive removal of methylene blue and malachite green from solutions. *Environmental Science and Pollution Research*, *24*(32), 25291–25308. https://doi.org/10.1007/s11356-017-0111-2

Oyewo, O. A., Mutesse, B., Leswifi, T. Y., & Onyango, M. S. (2019). Highly efficient removal of nickel and cadmium from water using sawdust-derived cellulose nanocrystals. *Journal of Environmental Chemical Engineering*, *7*(4), 103251. https://doi.org/10.1016/j.jece.2019.103251

Ranjbar, D., Raeiszadeh, M., Lewis, L., MacLachlan, M. J., & Hatzikiriakos, S. G. (2020). Adsorptive removal of Congo red by surfactant modified cellulose nanocrystals: a kinetic, equilibrium, and mechanistic investigation. *Cellulose*, *27*(6), 3211–3232. https://doi.org/10.1007/s10570-020-03021-z

Sahoo, T. R., & Prelot, B. (2020). Adsorption processes for the removal of contaminants from wastewater: The perspective role of nanomaterials and nanotechnology. *Nanomaterials for the Detection and Removal of Wastewater Pollutants*, 161–222. https://doi.org/10.1016/B978-0-12-818489-9.00007-4

Schroeder, L. R., Gentile, V. M., & Atalla, R. H. (2010). Nondegradative preparation of amorphous cellulose. *Journal*

of Wood Chemistry and Technology, *6*(1), 1–14. https://doi.org/10.1080/02773818608085213

Sun, B., Zhang, M., Hou, Q., Liu, R., Wu, T., & Si, C. (2016). Further characterization of cellulose nanocrystal (CNC) preparation from sulfuric acid hydrolysis of cotton fibers. *Cellulose*, *23*(1), 439–450. https://doi.org/10.1007/s10570-015-0803-z

Trache, D., Hussin, M. H., Haafiz, M. K. M., & Thakur, V. K. (2017). Recent progress in cellulose nanocrystals: Sources and production. *Nanoscale*, *9*(5), 1763–1786. https://doi.org/10.1039/c6nr09494e

Trache, D., Hussin, M. H., & Thakur, V. K. (2017). *Recent progress in cellulose nanocrystals: sources and production*. 1763–1786. https://doi.org/10.1039/c6nr09494e

Wanninayake, D. M. (2021). Comparison of currently available PFAS remediation technologies in water: A review. *Journal of Environmental Management*, *283*(September 2020), 111977. https://doi.org/10.1016/j.jenvman.2021.111977

Yin, J. J., Wahid, F., Zhang, Q., Tao, Y. C., Zhong, C., & Chu, L. Q. (2017). Facile Incorporation of Silver Nanoparticles into Quaternized Poly(2-(Dimethylamino)Ethyl Methacrylate) Brushes as Bifunctional Antibacterial Coatings. *Macromolecular Materials and Engineering*, *302*(6), 1–8. https://doi.org/10.1002/mame.201700069

Zhang, D., Luo, Q., Gao, B., Chiang, S. Y. D., Woodward, D., & Huang, Q. (2016). Sorption of perfluorooctanoic acid, perfluorooctane sulfonate and perfluoroheptanoic acid on granular activated carbon. *Chemosphere*, *144*, 2336–2342. https://doi.org/10.1016/j.chemosphere.2015.10.124

Zhang, H., Qian, Y., Chen, S., & Zhao, Y. (2019). Physicochemical characteristics and emulsification properties of cellulose nanocrystals stabilized O/W pickering emulsions with high -OSO3- groups. *Food Hydrocolloids*, *96*(May), 267–277. https://doi.org/10.1016/j.foodhyd.2019.05.023